JOURNAL GEOLOGICAL SOCIETY OF INDIA
Vol.78, December 2011, pp.501-509

Petrogenesis of Gabbro and Orthopyroxene Gabbro from the Phenai Mata Igneous Complex, Deccan Volcanic Province: Products of Concurrent Assimilation and Fractional Crystallization

K. R. HARI[1], N. V. CHALAPATHI RAO[2] and VIKAS SWARNKAR[1]
[1]Government V.Y.T.PG. Autonomous College, Durg, Chhattisgarh
[2]Centre of Advance Study in Geology, Banaras Hindu University, Varanasi – 221 005
Email: krharigeology@gmail.com

Abstract: We report the occurrence of orthopyroxene gabbro from the Phenai Mata Igneous Complex (containing thoeliitic and alkaline rocks) that occur within Deccan Traps. The P-T calculations based on two pyroxene thermometry vary from 8.5±1.0 kbar and 963±39 °C. These gabbroic rocks exhibit high Mg# (0.67 to 0.71). But their primary magma signature can be negated due to their high SiO_2 (> 50 wt %), low Ni (32-35 ppm) and Cr (105-182 ppm) contents. Further, simple fractional crystallization was not responsible for the modification of the magma. Modeling carried out using trace element concentrations revealed that concurrent assimilation and fractional crystallization (AFC) was responsible for the genesis of these rocks. Small pods of magma could have accumulated in the crustal portions and concurrent assimilation and fractional crystallization have taken place in the generation of gabbro and orthopyroxene gabbro in the present study area.

Keywords: Orthopyroxene, Deccan Traps, Concurrent Assimilation and Fractional Crystallization, Gabbro, Phenai Mata.

INTRODUCTION

The Deccan Traps are continental flood basalts that record immense accumulations of tholeiitic basaltic eruptions with an eruptive area of 1.5 x 10^6 km^2 (Fig. 1). Most intense pulse of volcanism occurred at 66.9±0.2 Ma, preceding the Cretaceous / Tertiary boundary (KTB, 65.2±0.2 Ma) (Chenet et al. 2007), approximately over a time period of 1.7 Ma. The lithology of Deccan Trap province is dominated by tholeiitic basalts and their derivatives. However, a wide ranging variety of rocks such as alkali – olivine basalt, rhyolites, nephelinites, lamprophyres, granites, gabbro, and carbonatites with limited geographic exposure and great petrogenetic significance have also been reported from different parts of western India such as Saurashtra – Kutch region and in the vicinity of the ENE–WSW trending Narmada - Son rift valley (e.g. Sukeshwala and Sethna, 1973; Krishnamurthy and Cox, 1977; Viladkar, 1981; Beane and Hooper, 1988; Greenough et al. 1998; Hari, 1998; Gwalani et al. 1993). Rare occurrences of 'orthopyroxene' in xenoliths from Kutch area (Karmalkar et al. 1999, 2008; Chandrasekharam and Vinod, 2000) and microliths of ferro–enstatite from dykes near Tapi rift (Chandrashekharam et al. 2000) have also been reported earlier from Deccan terrain. Chandrashekharam et al. (op. cit) concluded that the quench crystals of orthopyroxene are formed due to crustal contamination. In this paper, we report the occurrence of 'orthopyroxene bearing gabbro' (orthopyroxene gabbro) near the Phenai Mata Complex, the Deccan Traps and evaluate its possible genetic link with the gabbros exposed in this complex.

GEOLOGICAL SETTING

The Phenai Mata Igneous Complex (PMIC) is a plug like body whose emplacement is controlled by the Narmada rift (Kumar, 2003; Fig.1). It is a bi-modal complex comprising tholeiitic and alkaline magmatism represented by plutonic and volcanic rocks types. About two-thirds of PMIC is occupied by tholeiitic basalts and one-third by tholeiitic and alkaline plutonic series comprising gabbro dykelets of intrusive basalts, lamprophyres, microsyenite, granite and granophyre (Sukheswala and Sethna, 1969; 1973; Kumar, op.cit). Olivine bearing gabbros occupy the northeastern and eastern margins of the complex and small outcrops of the main hill. Kumar (1996a) established the stratigraphy of this igneous complex stating that phonolites,

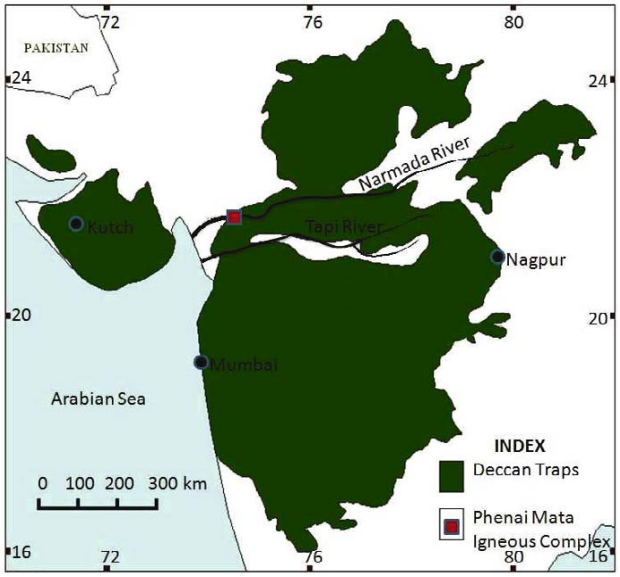

Fig.1. Map of Deccan traps showing the location of Phenai Mata Igneous Complex.

nephelinites, lamprophyres etc. are post-Deccan Traps, whereas the late phase of Deccan Traps event witnessed the emplacement of dolerite, microgranite, granophyre, gabbro etc at the Phenai Mata. Besides the Deccan Traps, the basement rocks in this area include Bagh sediments of Cretaceous age and the Pre-Cambrian granite-gneiss. Basu et al. (1993) based on $^{40}Ar/^{39}Ar$ dating, measured on an age of 65 Ma (late Deccan eruption) for the gabbro from this igneous complex. Gabbro bodies have been encountered on the northern and eastern part of the main hill (Fig. 2). Towards the east part of the main hill, a single isolated small hillock (longitude 73°53'02.1"E – 73°53'06.3"E and latitude 22°07'55"N – 22°08'01.7"N; 130 m above sea level) of orthopyroxene bearing gabbro is being reported for the first time in this paper.

PETROGRAPHY AND MINERAL CHEMISTRY

Mineralogically, both the rock types (gabbro and orthopyroxene gabbro) contain plagioclase, clinopyroxene, olivine, botite, opaques, minor amount of apatite and wth or without orthopyroxene. The gabbro containing orthopyroxene is being termed as "orthopyroxene gabbro" (nomenclature after Streckeisen, 1976) as the modal volume percentage of orthopyroxene (~8%) is minor in comparison to plagioclase and clinopyroxene (Table 1). There is a significant textural similarity between gabbro and orthopyroxene gabbro as both of them share sub-ophitic and ophitic textures (Fig.3A).

Chemical compositions of pyroxene, olivine, plagioclase and opaques were analysed using a CAMECA SX100 electron microprobe at the Institute of Mineralogy and Mineral Resources, Technical University of Claustal, Germany by one of us (NVCR). A beam current of 20nA acceleration voltage of 20kV and a beam diameter of 1 micron was used. Both natural as well as synthetic

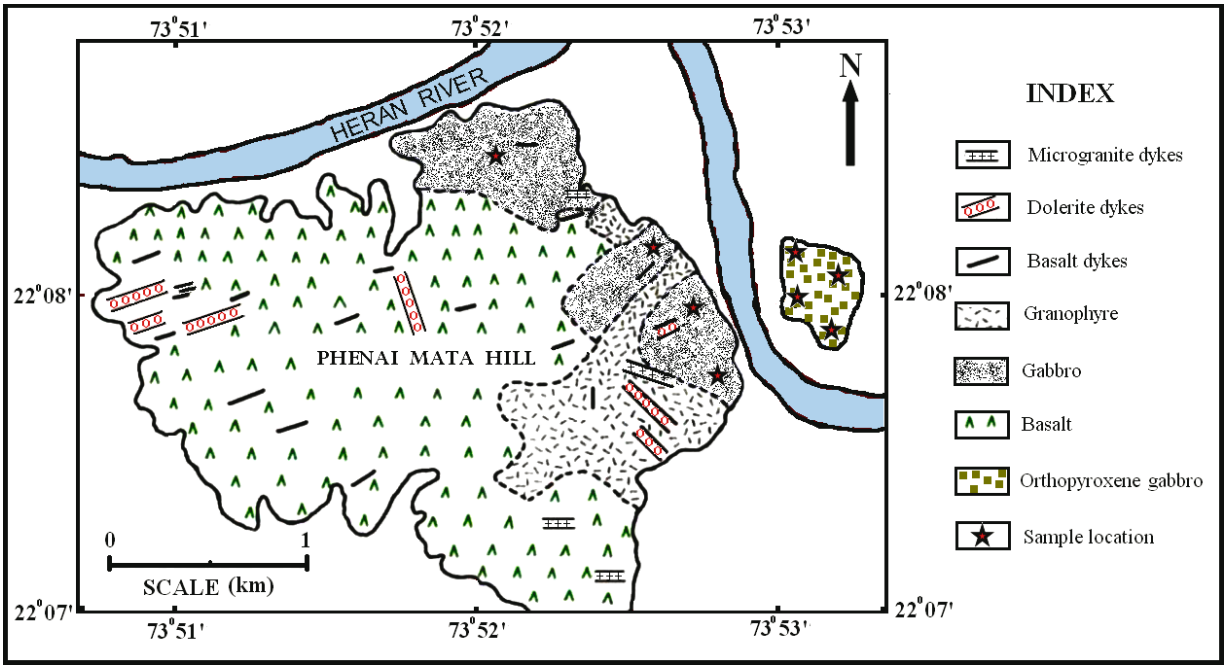

Fig.2. Geological map of Phenai Mata Igneous Complex (modified after Kumar et al. 1992).

Table 1. Modal percentage on volume basis of gabbro and orthopyroxene gabbro

Minerals	Gabbro				Orthopyroxene gabbro			
	PG-14	PG-20	PG 32	PG-41	PQ-11	PQ-23	PQ-34	PQ-42
Plagioclase	42	42	45	55	50	48	49	45
Clinopyroxene	36	34	35	31	22	23	23	16
Olivine	14	16	12	06	13	16	15	20
Orthopyroxene	Nil	Nil	Nil	Nil	7	6	7	12
Opaques	04	03	04	05	06	04	05	05
Biotite	03	04	04	01	02	03	01	02
Apatite	01	01	Nil	02	Nil	Nil	Nil	Nil

standards were employed and the obtained data is presented in Tables 2 and 3. Details of the analytical procedures are given in Torab and Lehman (2007).

Plagioclase (An_{51-57}) in the dominant constituent mineral in both gabbro and orthopyroxene gabbro. EPMA analyses of the feldspars reveal that the An content varied from 57 to 67 (Table 2; Fig. 4). However, one grain represents alkali feldspar (Or_{86}). Hari and Swarnkar (2011) reported similar type of alkali feldspar from the mesostasis of 'primitive picrite' rock from Kawant area. The modal volume percentage of clinopyroxene in gabbro is slightly higher than that of orthopyroxene gabbro (Table 1). In both the rocks, clinopyroxene is of augite composition which is also confirmed by the EPMA. Only minor chemical variations are noticeable in the clinopyroxene grains (Wo_{42-45}; En_{39-40}; Fs_{16-18}) (Table 3).

Orthopyroxene is confined only to orthopyroxene gabbro and its modal composition vary from 6 to 12. In most of the cases, orthopyroxene grains are seen as reaction rims around olivine (Fig.3B, C and D). However, some discrete grains are also noticeable in the sections. Orthopyroxene grains exhibit distinct pleochroism also (pink to green) compositionally, they show little chemical variations (Wo_{3-4}; En_{61-66}; Fs_{32-35}) (Table 3). The FeO(t) content in orthopyroxene found in the sample of PQ-23 of this area is ~20% which is comparable to the published value of Deer et al. (1992). Therefore, it is termed as ferro-enstatite. As the occurrence of orthopyroxene in Deccan volcanic province is rare, we plotted our orthopyroxene and clinopyroxene data along with the data published by Karmalkar et al. (2000) and Chandrashekram et al. (2000) in the pyroxene quadrilateral (Fig. 5) and found that the

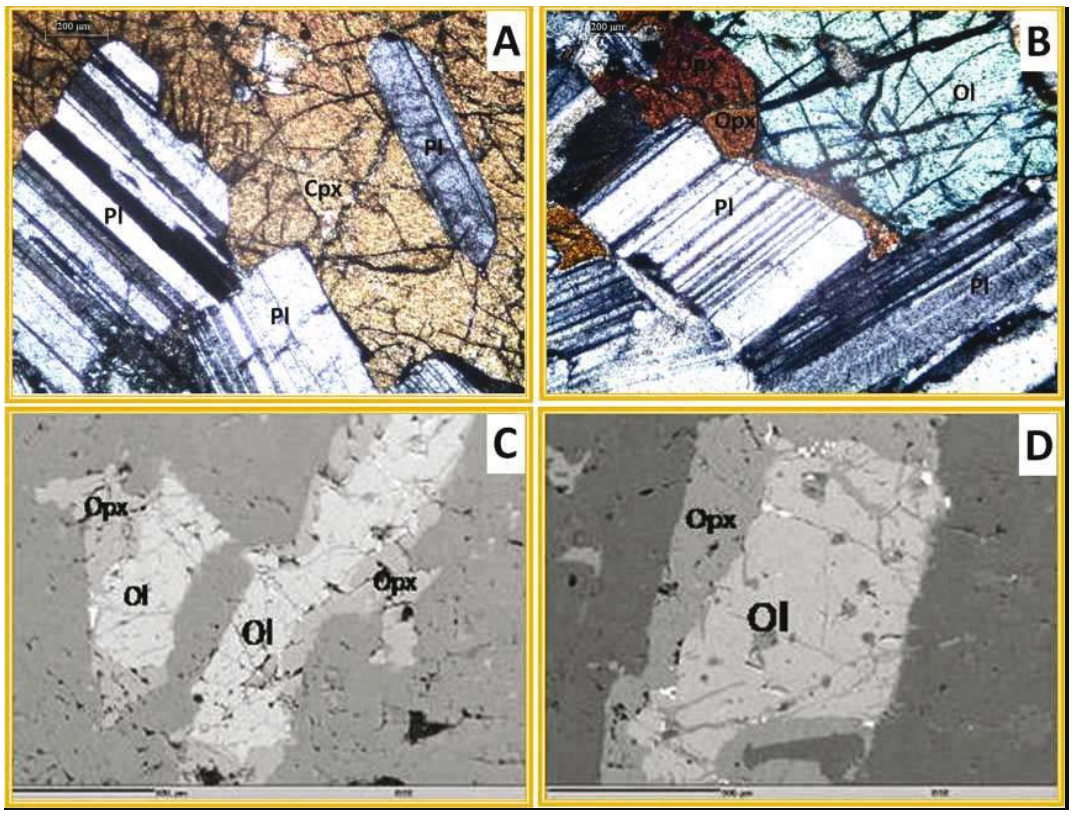

Fig.3. (A-B) Photomicrographs **(A)** depicting ophitic texture, **(B)** exhibiting olivine, orthopyroxene and olivine, in orthopyroxene gabbro. (**C and D**) BSE images showing orthopyroxene as reaction rim around olivine. Ol-Olivine, Opx-Orthopyroxene, Cpx-Clinopyroxene, Pl-Plagioclase.

Table 2. Mineral chemistry of feldspars from orthopyroxene gabbro

	1	2	3	4	5	6
SiO_2	54.64	52.21	51.84	51.94	51.94	64.81
TiO_2	0.05	0.05	0.06	0.07	0.06	0.06
Al_2O_3	29.32	30.62	30.98	30.80	30.59	19.28
Cr_2O_3	0.01	0.00	0.01	0.00	0.01	0.01
FeO	0.40	0.43	0.54	0.54	0.58	0.05
MnO	0.02	0.00	0.00	0.03	0.01	0.02
MgO	0.02	0.02	0.04	0.04	0.06	0.00
CaO	11.95	13.61	13.79	13.54	13.71	0.38
Na_2O	4.72	3.82	3.51	3.96	3.81	1.25
K_2O	0.29	0.21	0.41	0.38	0.37	13.83
NiO	0.01	0.00	0.00	0.00	0.00	0.00
Total	**101.43**	**100.96**	**101.17**	**101.30**	**101.14**	**99.70**
Formula (on the basis of 32 oxygen atoms)						
Si	9.759	9.415	9.345	9.360	9.375	11.897
Ti	0.007	0.007	0.009	0.009	0.008	0.009
Al	6.204	6.542	6.617	6.576	6.542	4.193
Cr	0.001	0.000	0.001	0.000	0.001	0.001
Fe	0.059	0.065	0.081	0.081	0.088	0.008
Mn	0.003	0.000	0.000	0.005	0.002	0.003
Mg	0.006	0.005	0.012	0.012	0.017	0.000
Ca	2.288	2.630	2.664	2.615	2.651	0.075
Na	1.634	1.335	1.225	1.383	1.335	0.446
K	0.066	0.049	0.094	0.088	0.085	3.239
Ni	0.001	0.000	0.000	0.000	0.000	0.000
Mol. Per cent						
Or	1.65	1.22	2.36	2.14	2.09	86.14
Ab	40.98	33.26	30.76	33.85	32.79	11.86
An	57.37	65.52	66.89	64.01	65.12	2.00

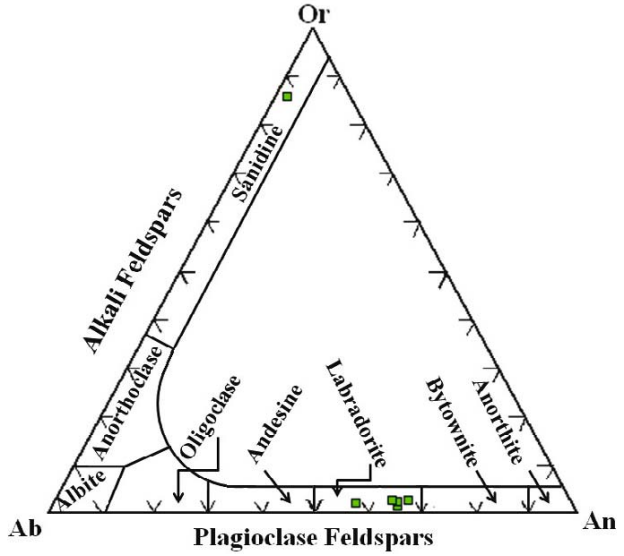

Fig.4. Mineral composition of feldspar in the orthopyroxene gabbro plotted on the Or-Ab-An diagram.

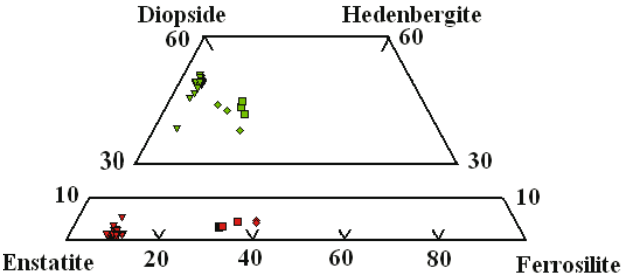

Fig.5. Mineral composition of the pyroxene from the present study (square), data from Chandrasekharam et al. (2000) and data from Karmalkar et al. (2000) plotted on the pyroxene quadrilateral.

pyroxene grains from the xenoliths of Kutch area are more Mg rich than those of the pyroxene grains which are seen as microliths in the basaltic dykes from Tapi rift and also from the orthopyroxene gabbro of the present study area.

Olivine grains have resorbed margin and Fo% varies from 58 to 61 (Table 3). Serpentinization is common along the rims and fractures of olivine. Ilmenite and magnetite (Table 3) are the opaque minerals identified in the orthopyroxene gabbro.

Sukheswala and Sethna (1969) reported variation in plagioclase (An_{50-20}), pyroxene (En_{75-53}), olivine (Fo_{75-45}) along with magnetite and biotite. Kumar (1996b) reported tholeiitic gabbro and alkali gabbro with a compositional variation in pyroxene ($Wo_{40}\ En_{45}\ Fs_{15}$ to $Wo_{47}\ En_{42}\ Fs_{11}$) in the latter and a restricted composition ($Wo_{49}\ En_{39}\ Fs_{11-12}$) in the former.

The P-T calculations with the RiM69_Ch03_two pyroxene_ P-T.xls software (Putirka, 2008) gave a temperature of 963±39 °C and pressure of 7.4 to 8.5±1.0 kbar for the orthopyroxene gabbro. Temperature and oxygen fugacity (magnetite-ilmenite geothermometry) calculated with the ILMAT excel worksheet (Lepage, 2003) gave a temperature of 632±9 °C which is lower than two pyroxene thermometric values and fO_2 of -20 to -19 (equations based on Andersen and Lindsley, 1985).

WHOLE ROCK GEOCHEMISTRY

Eight samples (four each of gabbro and orthopyroxene gabbro) analysed for major and trace elements concentrations using XRF and ICP-MS respectively at Wadia Institute of Himalayan Geology, Dehradun, India and are presented in Table 6. Concentrations of elements incompatible in olivine and hypersthenes are lower the orthopyroxene gabbro than in other gabbros, where as other elements (for e.g., Fe, Co, Ni, Mn, Mg, V) are in higher concentration in orthopyroxene gabbro. Both the rock types share a similar REE chondrite normalized pattern (Fig. 6) with a gentle slope. However, a slight positive Eu anomaly is seen in some samples indicating plagioclase accumulation.

Table 3. Mineral chemistry of pyroxene, olivine, ilmenite and magnetite from orthopyroxene gabbro

	Pyroxene									Olivine							Ilmenite		Magnetite	
	1	2	3	4	5	6	7	8	9	1	2	3	4	5	6	7	1	2	3	4
SiO_2	52.04	53.47	52.43	53.50	53.21	52.99	53.57	53.51	53.38	37.54	36.19	36.34	37.00	36.97	36.35	35.46	0.02	0.22	0.04	0.07
TiO_2	0.76	0.39	0.38	0.31	0.27	0.28	0.21	0.28	0.30	0.02	0.00	0.02	0.02	0.04	0.00	0.01	50.83	50.67	4.13	3.84
Al_2O_3	2.39	1.51	2.07	1.00	1.01	1.03	0.99	1.07	0.89	0.00	0.02	0.02	0.01	0.01	0.00	0.02	0.00	0.00	2.51	2.85
Cr_2O_3	0.04	0.00	0.01	0.01	0.01	0.01	0.02	0.00	0.02	0.01	0.01	0.00	0.01	0.00	0.01	0.39	0.01	0.01	0.07	0.05
FeO	10.98	10.15	9.68	19.80	19.67	20.03	20.12	20.18	21.37	33.49	33.17	33.05	32.88	33.34	34.10	33.10	45.37	45.72	87.17	86.86
MnO	0.22	0.21	0.23	0.38	0.33	0.35	0.36	0.34	0.37	0.37	0.38	0.38	0.37	0.37	0.37	0.32	0.73	0.54	0.19	0.12
MgO	13.91	14.12	13.53	23.03	22.96	23.09	22.78	22.63	20.70	28.94	29.15	29.81	29.64	29.39	28.87	25.48	2.15	2.07	0.49	0.54
CaO	20.01	21.13	21.36	1.28	1.35	1.44	1.38	1.39	1.83	0.04	0.01	0.04	0.03	0.06	0.04	0.09	0.01	0.22	0.01	0.00
Na_2O	0.31	0.27	0.30	0.02	0.01	0.04	0.02	0.00	0.04	0.02	0.02	0.00	0.02	0.06	0.00	0.04	0.00	0.01	0.02	0.05
K_2O	0.00	0.00	0.02	0.00	0.00	0.00	0.00	0.02	0.00	0.01	0.00	0.00	0.00	0.00	0.00	0.00	0.01	0.01	0.00	0.00
NiO	0.01	0.02	0.05	0.02	0.02	0.00	0.00	0.00	0.02	0.02	0.01	0.03	0.06	0.01	0.04	0.06	0.00	0.00	0.01	0.05
Total	**100.67**	**101.27**	**100.04**	**99.36**	**98.84**	**99.26**	**99.45**	**99.42**	**98.91**	**100.45**	**98.96**	**99.70**	**100.04**	**100.24**	**99.77**	**94.98**	**99.13**	**99.47**	**94.63**	**94.43**
	Formula (on the basis of 6 oxygen atoms)									Formula (on the basis of 4 oxygen atoms)							6 oxygen atoms		32 oxygen atoms	
Si	1.935	1.970	1.957	1.983	1.983	1.972	1.987	1.985	2.004	1.024	1.006	1.001	1.013	1.012	1.005	1.031	0.001	0.011	0.016	0.027
Ti	0.021	0.011	0.011	0.009	0.008	0.008	0.006	0.008	0.008	0.000	0.000	0.000	0.000	0.001	0.000	0.000	1.939	1.926	1.173	1.090
Al	0.105	0.066	0.091	0.044	0.044	0.045	0.043	0.047	0.040	0.000	0.001	0.001	0.000	0.000	0.000	0.001	0.000	0.000	1.124	1.277
Cr	0.001	0.000	0.000	0.000	0.000	0.000	0.001	0.000	0.000	0.000	0.000	0.000	0.000	0.000	0.000	0.009	0.000	0.000	0.021	0.014
Fe	0.341	0.313	0.302	0.614	0.613	0.623	0.624	0.626	0.671	0.764	0.771	0.761	0.753	0.763	0.789	0.805	1.925	1.933	27.565	27.461
Mn	0.007	0.007	0.007	0.012	0.010	0.011	0.011	0.011	0.012	0.009	0.009	0.009	0.009	0.009	0.009	0.008	0.031	0.023	0.061	0.038
Mg	0.771	0.775	0.752	1.273	1.275	1.280	1.259	1.251	1.158	1.176	1.207	1.224	1.209	1.199	1.190	1.104	0.163	0.156	0.278	0.305
Ca	0.797	0.834	0.854	0.051	0.054	0.057	0.055	0.055	0.074	0.001	0.000	0.001	0.001	0.002	0.001	0.003	0.001	0.012	0.002	0.001
Na	0.022	0.019	0.021	0.001	0.001	0.003	0.002	0.000	0.003	0.001	0.001	0.000	0.001	0.003	0.000	0.002	0.000	0.001	0.012	0.033
K	0.000	0.000	0.001	0.000	0.000	0.000	0.000	0.001	0.000	0.000	0.000	0.000	0.000	0.000	0.000	0.000	0.000	0.000	0.000	0.000
Ni	0.000	0.001	0.001	0.001	0.001	0.000	0.000	0.000	0.001	0.000	0.000	0.001	0.001	0.000	0.001	0.001	0.000	0.000	0.003	0.016
	Atomic percentages																			
Ca	41.76	43.40	44.75	2.62	2.77	2.93	2.83	2.85	3.89	-	-	-	-	-	-	-	-	-	-	-
Mg	40.37	40.34	39.42	65.69	65.66	65.29	64.97	64.75	60.85	60.3	60.8	61.4	61.3	60.8	59.9	57.6	-	-	-	-
Fe	17.87	16.26	15.83	31.69	31.58	31.78	32.20	32.40	35.26	39.2	38.8	38.2	38.2	38.7	39.7	42.0	-	-	-	-
Mn	-	-	-	-	-	-	-	-	-	0.5	0.5	0.5	0.5	0.5	0.5	0.4	-	-	-	-

Table 6. Major element analyses (in wt%) and trace element concentrations (in ppm) of gabbro (PG-14, PG-20, PG-32, PG-41) and orthopyroxene gabbro (PQ-11, PQ-23, PQ-34, PQ-42)

	PG-14	PG-20	PG-32	PG-41	PQ-11	PQ-23	PQ-34	PQ-42
SiO_2	50.70	51.12	51.07	51.13	48.40	47.45	47.32	47.34
TiO_2	0.64	0.66	0.66	0.82	0.69	0.70	0.69	0.75
Al_2O_3	20.70	19.95	19.77	19.48	18.70	18.75	18.15	17.22
Fe_2O_3	5.57	5.64	5.29	6.52	11.27	11.51	11.64	12.85
MnO	0.09	0.09	0.09	0.10	0.14	0.14	0.15	0.16
MgO	5.53	5.62	5.80	5.93	7.39	7.52	7.91	8.20
CaO	13.07	13.23	13.11	13.05	11.57	11.61	11.48	11.16
Na_2O	2.49	2.56	2.49	2.52	2.19	2.19	2.19	2.09
K_2O	0.99	0.99	1.10	0.94	0.47	0.46	0.45	0.49
P_2O_5	0.26	0.25	0.13	0.08	0.08	0.04	0.04	0.04
SUM	**100.05**	**98.86**	**98.28**	**99.57**	**100.89**	**99.87**	**99.53**	**99.77**
Mg#	0.69	0.69	0.71	0.67	0.59	0.59	0.60	0.58
La	26.91	35.70	22.50	18.10	10.50	10.00	10.53	13.43
Ce	51.81	70.40	43.20	35.40	18.91	18.32	19.50	25.53
Pr	5.99	7.94	4.95	4.10	2.11	2.10	2.30	2.92
Nd	22.10	28.30	17.30	14.43	7.40	7.60	8.40	10.85
Sm	3.70	4.84	3.24	2.56	1.46	1.44	1.61	2.02
Eu	1.13	1.56	1.20	1.09	0.60	0.59	0.66	0.85
Gd	3.73	4.77	3.35	2.61	1.52	1.46	1.72	2.12
Tb	0.53	0.65	0.51	0.39	0.22	0.21	0.25	0.31
Dy	2.91	3.55	2.72	2.16	1.23	1.20	1.40	1.78
Ho	0.58	0.75	0.56	0.44	0.26	0.26	0.30	0.36
Er	1.50	1.87	1.48	1.20	0.69	0.68	0.79	0.93
Tm	0.22	0.29	0.22	0.19	0.10	0.10	0.12	0.15
Yb	1.43	1.80	1.50	1.18	0.67	0.63	0.76	0.95
Lu	0.21	0.26	0.22	0.19	0.10	0.10	0.12	0.14
Ba	273.47	301.68	259.07	245.37	254.96	256.00	240.87	277.65
Cr	105.64	108.35	181.80	173.30	51.08	50.13	89.20	85.86
V	87.99	96.63	96.26	152.02	251.19	235.11	237.11	256.31
Co	28.24	26.55	26.96	34.06	54.06	51.57	55.50	57.69
Ni	32.27	35.19	34.70	35.15	63.81	64.67	65.13	72.55
Rb	25.49	26.62	28.57	20.65	13.51	12.27	8.97	13.46
Sr	526.24	528.41	505.43	501.46	546.08	547.42	516.56	492.65
Y	19.18	19.63	16.58	16.31	5.66	6.25	7.95	7.51
Zr	91.18	95.96	99.84	105.50	52.00	48.25	47.29	55.49
Nb	20.15	18.88	19.02	21.92	9.73	10.64	10.70	11.57

DISCUSSION

Primary magmas in equilibrium with upper mantle mineralogy should have high Mg# values (> 0.70), high Ni (> 400-500 ppm), high Cr (> 1000 ppm) and SiO_2 not exceeding 50% (Wilson, 1989, p-22). Krishnamurthy and Cox, (1977); Beane and Hooper, (1988); Peng and Mahoney, (1995); Greenough et al. (1998); Krishnamurthy et al. (2000); Hari and Swarnkar (2011) have reported basalts exhibiting primary/primitive nature from different parts of Deccan Traps. In the present study, the gabbroic rocks exhibit high Mg# value (0.67 to 0.71) but their SiO_2 wt% are relatively high (50.7 to 51.13) (Table 6). Further, the high incompatible trace elemental concentrations (500-528 ppm Sr; 250-300 ppm Ba; 91-105 ppm Zr) and low Ni (32-35 ppm) and Cr (105-182 ppm) concentrations (Table 6) negate their primary magma signature and suggest that the

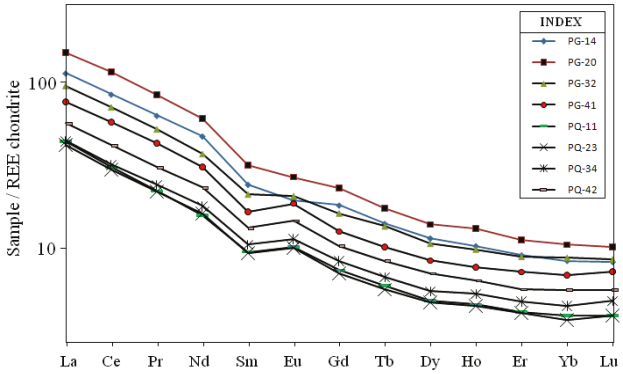

Fig.6. Chondrite normalized REE (normalizing values after Sun and Mc Donough, 1989) patterns of gabbro (PG-14, PG-20, PG-32, PG-41) and orthopyroxene gabbro (PQ-11, PQ-23, PQ-34, PQ-42).

modification of the magma by some petrogenetic process might have taken place.

Fractional crystallization is an important process for the modification of magma and can be evaluated with the help of variation diagrams. The decreasing trends of SiO_2 and Al_2O_3 (Fig.7) and increasing Ni and Cr contents with MgO (Table 6) point towards the importance of olivine and pyroxene fractionation. No specific pattern is noticeable in

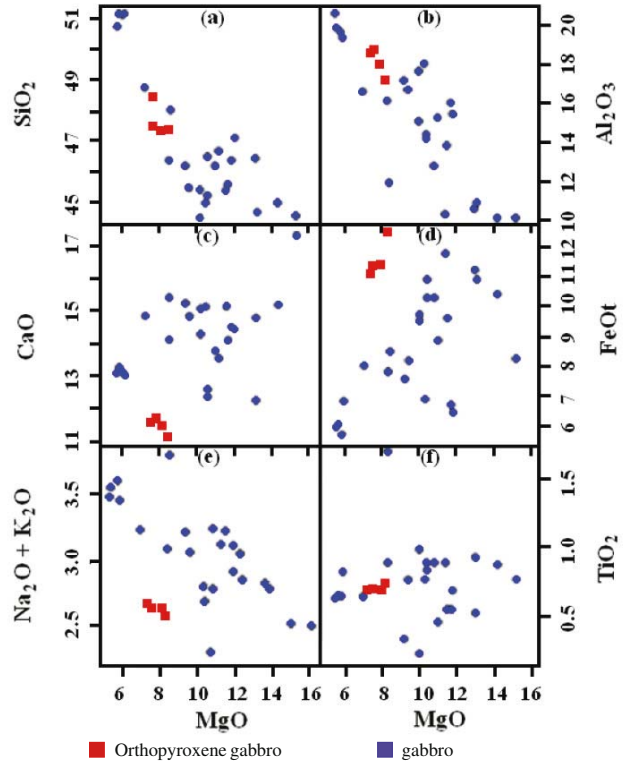

Fig.7. Major element variation diagrams of gabbro and orthopyroxene gabbro. Geochemical data of gabbro by Kumar (2003) is also incorporated in the figure.

case of CaO, TiO_2, Fe_2O_3 and Na_2O+K_2O when plotted against MgO (Fig. 7). Plagioclase fractionation did not play an important role in the whole petrogenesis which is evident from the absence of negative Eu anomaly in the chondrite normalized REE diagram (Fig. 6). However, in the present case, simple fractional crystallization could not modify these magmas as the incompatible trace elemental concentrations in the gabbro and orthopyroxene gabbro of the present region are high.

Concurrent assimilation and fractional crystallization (AFC) is an important process for the modification of the magma and De Paolo (1981) developed an equation for trace elements and isotopes for evaluating this process. In order to evaluate the AFC process, the qualitative and quantitative analyses of the fractionating minerals are to be taken into consideration. Vijaya Kumar et al. (2010) while evaluating the AFC process in Deccan Traps considered plagioclase as the main fractionating mineral followed by clinopyroxene, olivine, magnetite, ilmenite and apatite.

An attempt has been made to analyze the role of AFC in the generation of gabbro and orthopyroxene gabbro taking 45 % olivine, 35% clinopyroxene, 15% plagioclase and 5% magnetite as the fractionating minerals. Mineral/melt partition coefficient values are after Claeson and Meurer (2004). The contaminant is taken as the average upper crustal values from Rudnick and Gao (2003). As no gabbroic magma with primitive / primary signature has not been reported yet from Phenai Mata area, trace element concentrations of a gabbroic dyke having similar major elemental concentrations, with low incompatible elemental concentrations and with primitive signatures (RKV 328; Vijaya Kumar and Rathna, 2008) is taken as the original magma for calculations. The Rb verses Rb/Nb diagram (Fig.8) clearly shows that the average gabbro and orthopyroxene gabbro are not generated by perfect fractional crystallization (r = 0) but with a slightly higher ratio of assimilation to fractional crystallization (r = 0.025). Keeping r = 0.025, REE modeling (Fig. 9) were also carried out and has been found that the orthopyroxene gabbro and gabbro can be formed by AFC.

Whilst tracing the evolution of Deccan volcanic province mainly in Kutch region which is proximal to two conjugate Narmada and Cambay rift systems, Karmalkar et al. (2008) concluded that magma underplating is the common phenomenon in this region and the magma chambers beneath Kutch occurs as plexus of interconnected dykes and magma pockets from which this magma was periodically expelled. Vijaya Kumar et al. (2010) stressed that detailed traverses across small stratigraphic intervals are needed in unraveling complex mantle and magma chamber processes relevant to genesis of Deccan Traps. They further argued that the parental melts segregated within lower crustal magma chamber(s) and underwent the first stage fractional crystallization dominated by olivine and clinopyroxene (±spinel), thus producing Fe- and Al-rich tholeiitic melts. These fractionated melts migrated to upper crustal regions where the melts again ponded, but in shallow level magma chambers where concurrent assimilation and fractional crystallization took place. In the present area, small pods of magma could have accumulated in the crustal portions and concurrent assimilation and fractional crystallization have taken place giving rise to gabbro and orthopyroxene gabbro.

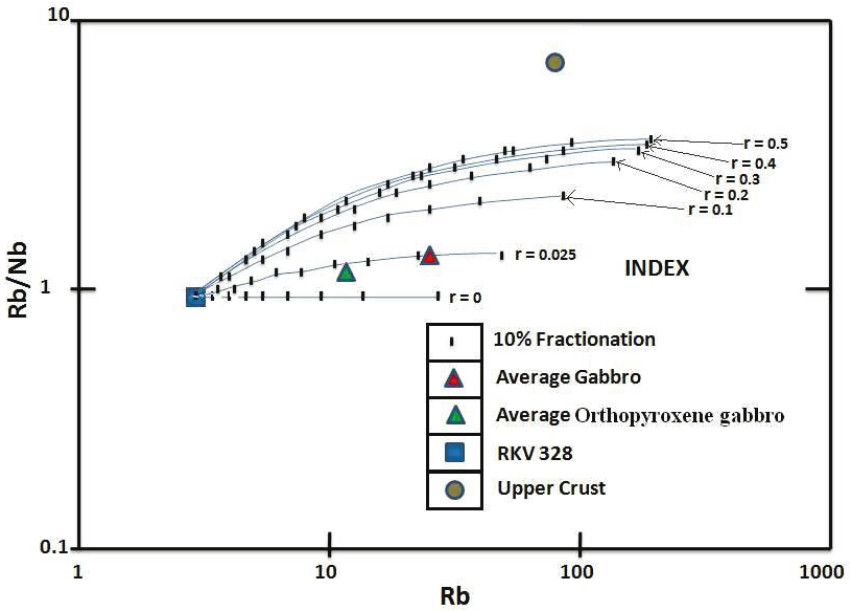

Fig.8. Rb vs Rb/Nb diagram depicting the role of concurrent assimilation and fractional crystallization. RKV 328 sample is taken as the parental magma. 'r' is the ratio of the rate of assimilation to the rate of fractional crystallization 'F' values calculated with varying 'r' are plotted in the figure. The average values of gabbro and orthopyroxene gabbro fall above the perfect fractional crystallization line (r = 0) indicating that they were subjected to AFC.

Their close association in the field and similarities in texture, mineralogy, REE chondrite patterns and mantle normalized patterns of gabbro and orthopyroxene gabbro point a close genetic link between these two rock types. Experimental studies have shown that in many basalts crystallizing at 10-20 kbar, orthopyroxene disappears from the crystallization sequence after

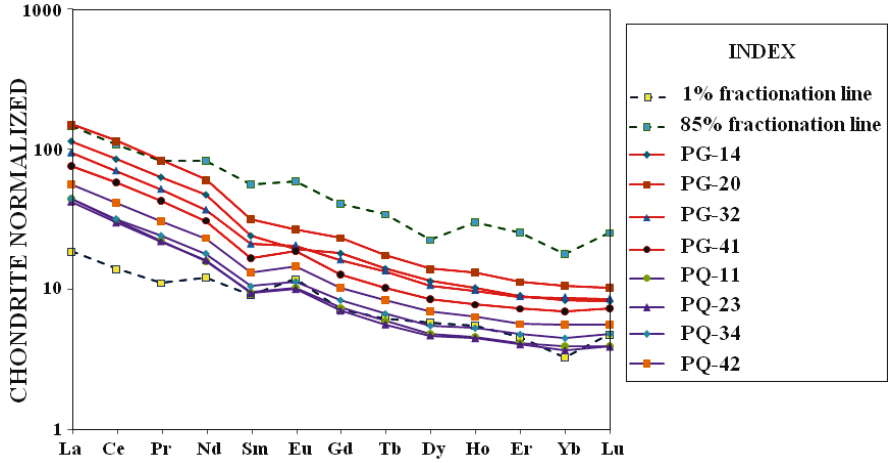

Fig.9. Chondrite normalized (Nakamura, 1974) REE diagram of the results of the modeling of concurrent assimilation and fractional crystallization. For calculating the fractionation trends, r is kept as 0.025. Gabbro (PG-14, PG-20, PG-32, PG-41) and orthopyroxene gabbro (PQ-11, PQ-23, PQ-34, PQ-42). Please refer the text for details.

clinopyroxene and olivine and if orthopyroxene has not joined the crystallization sequence before clinopyroxene, it never does, thereby suggesting that ol + cpx crystallization drives residual liquids away from opx saturation (Stolper, 1980).

Acknowledgements: We are thankful to Dr. Loÿc Vanderkluyse for his critical suggestions on an earlier version of the manuscript. Thanks are due to the anonymous reviewer for his constructive suggestions for improving the manuscript and to Dr. Keith Putirka for the fruitful discussions. We thank Department of Science and Technology, New Delhi, India for providing the research grant (ESS/16/295/2006).

References

ANDERSEN, D.J. and LINDSLEY, D.H. (1985) New (and final!) models for the Ti-magnetite/ilmenite geothermometer and oxygen barometer. Abstract AGU 1985 Spring Meeting Eos Transactions. Amer. Geophys. Union, v.66 (18), p.416.

BASU, A.R., RENNE, P.R., DAS GUPTA, D.K., TEICHMA, F. and POREDA, R.J. (1993) Early and late alkali igneous pulses and a high – ^{3}He plume origin for the Deccan flood basalts. Science, v.261, pp.902-906.

BEANE, J.E. and HOOPER, P.R. (1988) A note on the picrite basalts of the western Ghats, Deccan traps, India. *In* : Subbaro K. V (Ed) Deccan flood basalts. Geol. Soc. of India, Memoir, v.10, pp.117-133.

CHANDRASEKHARAM, D., VASELLI, O., SHETH, H.C. and KESHAV, S. (2000) Petrogenetic significance of ferro-enstatite orthopyroxene in basaltic dikes from the Tapi rift, Deccan flood basalt province, India. Earth Planet. Sci. Lett., v.179, pp.469-476.

CHANDRASEKHARAM, D. and VINOD, K.C. (2000) Clinopyroxinite xenoliths from Deccan Trap lavas of Kutch and Mumbai. Curr. Sci., v.78, pp.607-610.

CHENET, A.L., QUIDELLEUR, X., FLUTEAU, F., COURTILLOT, V. and Bajpai, S. (2007) ^{40}K–^{40}Ar dating of the main Deccan large igneous province: further evidence of KTB age and short duration. Earth Planet. Sci. Lett., v.263, pp.1-15.

CLAESON, D.T. and MEURER, W.P. (2004) Fractional crystallization of hydrous basaltic ''arc-type'' magmas and the formation of amphibole-bearing gabbroic cumulates, Contrib. Mineral. Petrol., v.147, pp.288-304.

DEER, W.A., HOWIE, R.A. and ZUSSMAN, J. (1992). An introduction to Rock-forming minerals, 2nd ed. New York, Wiley.

DE PAOLO, D.J. (1981) Trace element and isotopic effects of combined wallrock assimilation and fractional crystallisation. Earth Planet. Sci. Lett., v.53, pp.189-202.

GREENOUGH, J.D., HARI, K.R., CHATTERJEE, A.C. and SANTOSH, M. (1998) Mildly alkaline basalts from Pavagadh Hill, India: Deccan flood basalts with an asthenospheric origin. Mineral. Petrol., v.62, pp.223-245.

GWALANI, L.G., ROCK, N.M.S., CHANG, W.J., FERNANDEZ, S., ALLEGRE, C.J. and PRINZOHOFER, A. (1993) Alkaline rocks and carbonatites of Amba Dongar and adjacent Areas, Deccan Igneous Province. Gujarat, India: Geology, petrography and petrochemistry. Mineral. Petrol., v.47, pp.219-253.

HARI, K.R. (1998) Mineralogical and Petrological Studies of the Lamprophyres around Chhaktalao area, Madhya Pradesh. Jour.

Geol. Soc. India., v.51, pp.28-30.

HARI, K.R. AND SWARNKAR, VIKAS (2011) Petrogenesis of basaltic and doleritic dykes from Kawant, Chhotaudepur province, Deccan Traps. *In:* Rajesh Srivastava (Ed.), Dyke swarms: keys to geodynamic interpretations. Springer Publications, pp.283-299.

KARMALKAR, N.R., DURAISWAMI, R.A., GRIFFIN, W.L. and O'REILLY, S.Y. (1999) Enigmatic orthopyroxene-rutile-spinel intergrowth in the mantle xenoliths from Kutch, India. Curr. Sci., v.76, pp.687-692.

KARMALKAR, N.R., GRIFFIN, W.L. and O'REILLY, S.Y. (2000) Ultramafic Xenoliths from Kutch, Northwest India: Plume-Related Mantle Samples? Internat. Geol. Rev., v.42, pp.416-444.

KARMALKAR, N.R., KALE, M.G., DURAISWAMI, R.A. and JONALGADDA, M. (2008) Magma underplating and storage in the crust-building process beneath the Kutch region, NW India. Curr. Sci., v.94, pp.1582-1588.

KRISHNAMURTHY, P. and COX, K. G. (1977) Picrite basalts and related lavas from the Deccan Traps of western India. Contrib. Mineral. Petrol., v.62, pp.53-75.

KRISHNAMURTHY, P., GOPALAN, K. and MACDOUGALL, J.D. (2000) Olivine compositions in picrite basalts and the Deccan volcanic cycle. Jour. Petrol., v.41 No.7, pp.1057-1069.

KUMAR, SANTOSH (1996a) Geochemical speciation of Phenai Mata Igneous Complex, Baroda district, Gujarat. Jour. Scientific Res., v.46, pp.207-218.

KUMAR, SANTOSH (1996b) Chemistry of clinopyroxene from subalkaline and alkaline rocks of Phenai Mata igneous complex, Baroda district, Western India. Jour. Geol. Soc. India, v.48, pp.547-558.

KUMAR, SANTOSH (2003) Pearce Element Ratios applied to model basic rock members of Phenai Mata Igneous Complex, Baroda district, Gujarat. Jour. Geol. Soc. India, v.61, pp.565-572.

LEPAGE, L.D. (2003) ILMAT: an Excel worksheet for ilmenite–magnetite geothermometry and geobarometry. Computers & Geosciences, v.29, pp.673-678.

NAKAMURA, N. (1974) Determination of REE, Ba, Fe, Mg, Na and K in carbonaceous and ordinary chondrites. Geochim. Cosmochim. Acta., v.38, pp.757-773.

PENG, Z.X. and MAHONEY, J.J. (1995) Drillhole lavas from the northwestern Deccan Traps, and the evolution of Reunion hotspot mantle. Earth Planet. Sci. Lett., v.134, pp.169-185.

PUTIRKA, K. (2008) Thermometers and barometers for volcanic systems. *In:* K. Putrika and F. Tepley (Eds.), Minerals, inclusions and volcanic processes. Reviews in Mineralogy and Geochemistry, Mineral. Soc. Amer., v-69, pp 61-120.

STOLPER, E. (1980) A phase diagram for Mid-Oceanic Ridge Basalts: Preliminary result and implications for petrogenesis. Contrib. Mineral. Petrol., v.74, pp.13-27.

STRECKIESEN, A. (1976) To each plutonic rock its proper name. Earth Sci. Rev., v.12, pp.1-33.

SUKHESWALA, R.N. and SETHNA, S.F. (1969) Layered gabbro of the igneous complex of Phenaimata, Gujarat State. Jour. Geol. Soc. India, v.10, pp.117-187.

SUKHESWALA, R.N. and SETHNA, S.F. (1973) Oversaturated and undersaturated differentiates in the tholeiitic igneous complex of Phenai Mata,Baroda district,Gujarat state, India. Neues Jahrbuch für Mineralogie Abhandlungen v.118, pp.159-176.

SUN, S.S. and MCDONOUGH, W.F. (1989) Chemical and isotopic systematics of oceanic basalts: implications for mantle composition and processes. Geol. Soc. London Spec. Publ., v.42, pp.313-345.

TORAB, F.M. and LEHMANN, B. (2007) Magnetite – apatite deposits of the Bafq district, Central Iran: apatite geochemistry and monazite geochemistry. Mineral. Mag., v.71, pp.347-367.

VIJAYA KUMAR and RATHNA, K. (2008) Geochemistry of the mafic dykes in the Prakasam Alkaline Province of Eastern Ghats Belt, India: Implications for the genesis of continental rift-zone magmatism. Lithos, v.104, pp.306-326.

VIJAYA KUMAR, KOPPARAPU, CHAVAN, CHAKRADHAR, SAWANT, SARIPUT, NAGA RAJU, K., KANAKDANDE, PRACHITI, PATODE, SANGITA., DESHPANDE, KRISHNA., KRISHNAMACHARYULU, S.K.G., VAIDESWARAN, T. and BALARAM. V. (2010) Geochemical investigation of a semi-continuous extrusive basaltic section from the Deccan Volcanic Province, India: implications for the mantle and magma chamber processes. Contrib. Mineral. Petrol., v.159, pp.839-862.

VILADKAR, S.G. (1981) The carbonatites of Amba Dongar, Gujarat, India. Indian Mineralogist, Sukheswala Volume, pp.130-135.

WILSON, M. (1989) Igneous Petrogenesis, London, Unwin Hyman, p.465.

(Received: 14 April 2010; Revised form accepted: 3 March 2011)